Title

Granulocyte-Macrophage Colony-Stimulating Factor Influence on Soluble and Membrane-Bound ICOS in Combination with Immune Checkpoint Blockade.

Journal

Cancer Immunology Research, 11(8)

Authors

Li, Xiaoyu
Li, Jingjing
Zheng, Yue
et al.

Publication Date

2023-08-03

DOI

10.1158/2326-6066.CIR-22-0702

Peer reviewed

Granulocyte–Macrophage Colony-Stimulating Factor Influence on Soluble and Membrane-Bound ICOS in Combination with Immune Checkpoint Blockade

Xiaoyu Li[1,2,3], Jingjing Li[1,2,3], Yue Zheng[4], Sandra J. Lee[4], Jun Zhou[1,2,3], Anita Giobbie-Hurder[2,3,4], Lisa H. Butterfield[5], Glenn Dranoff[6], and F. Stephen Hodi[1,2,3]

ABSTRACT

With the successful development of immune checkpoint blockade, there remains the continued need to improve efficacy and decrease toxicities. The addition of granulocyte–macrophage colony-stimulating factor (GM-CSF) to ipilimumab has previously demonstrated both an improvement in efficacy and decrease in the incidence of high-grade adverse events. $ICOS^+CD4^+$ or $ICOS^+CD8^+$ peripheral blood T cells are significantly greater in the patients treated with ipilimumab plus GM-CSF than in the patients treated with ipilimumab alone. To better understand the effects of GM-CSF on inducible T-cell costimulator (ICOS) and clinical outcomes, the relative roles of identified soluble ICOS and membrane-bound ICOS were evaluated. The ICOS splice variant was secreted and found to have immunologic suppressive effects. Changes in soluble ICOS splice variant levels in treated patients correlated with clinical outcomes. GM-CSF enhanced membrane-bound ICOS in an IL12-dependent manner but did not increase soluble ICOS levels. Whereas soluble ICOS plays a role in immune suppression, GM-CSF efficacy involves increasing membrane-bound ICOS and induction of dendritic cell development. Thus, soluble ICOS splice variants may be used as a biomarker for GM-CSF and immune checkpoint blockade–based therapies.

Introduction

Inducible T-cell costimulator (ICOS), also known as CD278, was identified as a member of the CD28–CTLA-4 T-cell costimulator subfamily of B7 superfamily costimulatory molecules (1–3). In contrast to CD28, which is expressed constitutively on both naïve and activated T cells, ICOS expression is induced on T cells only upon TCR cross-linking (1, 4–6). ICOS receptor engagement by its specific ligand, ICOSL (B7H/B7RP-1; refs. 4, 7) promotes T-cell differentiation, activation, and proliferation (5, 8, 9). A recent clinical study shows that dendritic cells (DC) from melanoma patients have reduced expression of membrane-bound and soluble ICOSL resulting from defective intrinsic NF-kB signaling, which correlates with the tumor-specific T-cell immune responses and patient clinical outcomes (10). A mouse tumor model of melanoma has provided experimental evidence that antitumor T-cell responses elicited by anti–CTLA-4 are significantly impaired in the absence of ICOS (11), suggesting that ICOS/ICOSL signaling is required for the optimal effect of cancer immunotherapy by immune checkpoint blockade.

Two isoforms of human ICOS have been identified, full-length ICOS (ICOS-FL; ref. 1) and an alternatively spliced variant (12). Soluble ICOS (sICOS) has been evaluated in patients with autoimmune disease (13–16). Upregulation of membrane-bound ICOS on peripheral blood T cells and downregulation of serum levels of sICOS are found in patients with neuromyelitis optica spectrum disorder (NMOSD) compared with healthy donors (13). Nevertheless, the involvement of sICOS in patients with malignant tumors has not been extensively studied. Serum levels of sICOS may regulate antitumor immune responses and could potentially be used as a biomarker for tumor immunity.

Preclinical mouse models, as well as clinical studies, have shown the role of granulocyte–macrophage–colony-stimulating factor (GM-CSF) in augmenting antitumor immunity in combination with immunotherapy, either through systemic administration of GM-CSF or by vaccination with irradiated autologous tumor cells genetically engineered to secrete GM-CSF, leading to enhanced tumor-specific T-cell activation and tumor destruction (17–23). In a randomized phase II trial [Eastern Cooperative Oncology Group (ECOG) 1608] of ipilimumab with or without GM-CSF, the addition of GM-CSF to CTLA-4 blockade prolongs overall survival and reduces toxicity in patients with metastatic melanoma. Notably, flow cytometry data demonstrate that the increased percentages of $ICOS^+CD4^+$ or $ICOS^+CD8^+$ peripheral blood T cells are significantly greater in the patients treated with ipilimumab plus GM-CSF than in the patients treated with ipilimumab alone (21). The present study sought to clarify the immunologic effects of GM-CSF on ICOS induction and the potential role of sICOS on clinical outcomes.

Materials and Methods

Cell lines

CHO-K1 cells (CCL-61) were purchased from the ATCC and maintained in Ham's F-12K (Kaighn's) Medium (Thermo Fisher Scientific, 21127022) supplemented with 10% fetal bovine serum (FBS, Thermo Fisher Scientific, 10437028), 100 U/mL penicillin, and

[1]Department of Medical Oncology, Dana-Farber Cancer Institute, Boston, Massachusetts. [2]Melanoma Division, Dana-Farber Cancer Institute, Boston, Massachusetts. [3]Center for Immuno-Oncology, Dana-Farber Cancer Institute, Boston, Massachusetts. [4]Department of Data Sciences, Dana-Farber Cancer Institute, Boston, Massachusetts. [5]Parker Institute for Cancer Immunotherapy and University of California San Francisco, San Francisco, California. [6]Immuno-Oncology, Novartis Institutes for Biomedical Research, Cambridge, Massachusetts.

Corresponding Author: F. Stephen Hodi, Dana-Farber Cancer Institute, 450 Brookline Avenue, Boston, MA 02215. Phone: 617-632-5053; E-mail: Stephen_hodi@dfci.harvard.edu

Cancer Immunol Res 2023;11:1100–13

doi: 10.1158/2326-6066.CIR-22-0702

100 μg/mL streptomycin (Thermo Fisher Scientific, 15140122). 293T cells (CRL-3216) were purchased from ATCC and maintained in DMEM (Thermo Fisher Scientific, 10313039) supplemented with 10% FBS, 100 U/mL penicillin, and 100 μg/mL streptomycin. All cell lines were frozen at passages 2 to 5 after purchase. Experiments were performed using passages 3 to 15 after removal from liquid nitrogen. *Mycoplasma* was routinely tested using the Mycoplasma Detection Kit (Millipore Sigma). Cell line authentication was done by ATCC.

Ethics approval and consent to participate

The collection and use of patient samples were complied with the Declaration of Helsinki and approved by the Institutional Review Board of the Dana-Farber/Harvard Cancer Center, Cancer Therapy Evaluation Program, and ECOG-American College of Radiology Imaging Network, and informed written consent was obtained from patients.

Human peripheral blood mononuclear cells isolation and DC generation

All human studies were approved by the Institutional Review Board of the Dana-Farber/Harvard Cancer Center. Human peripheral blood mononuclear cells (PBMC) were isolated from the peripheral blood of 12 healthy donors by Ficoll-Hypaque (Sigma-Aldrich) density gradient centrifugation. $CD14^+$ monocytes were purified from PBMCs of healthy donors by positive selection using CD14 magnetic microbeads (Miltenyi Biotec, 130-050-201) and MACS separation columns (Miltenyi Biotec, 130-042-401) following the manufacturer's instructions (Miltenyi Biotec). The components of the MACS buffer: 1X PBS, pH 7.2 (Thermo Fisher Scientific), 0.5% bovine serum albumin (BSA, Millipore Sigma), 2 mmol/L EDTA (Thermo Fisher Scientific). 3 mL of the MACS buffer was used for cell wash, and 0.5 mL was used for cell resuspension. The purity of the isolated $CD14^+$ cells was above 95%, determined by flow cytometry. $CD14^+$ cells were cultured for 6 days in a 24-well tissue culture plate at a concentration of 2×10^5 cells/mL in complete RPMI-1640 medium (RPMI-1640 medium, 10% FBS, 100 U/mL penicillin, and 100 μg/mL streptomycin) alone; in complete medium supplemented with GM-CSF (50 ng/mL, R&D Systems) plus IL4 (5 ng/mL, R&D Systems) and control IgG (10 μg/mL, BioLegend); in complete medium supplemented with GM-CSF (50 ng/mL) plus IL4 (5 ng/mL) and anti–GM-CSFR alpha (CD116, clone 4H1, 10 μg/mL, BioLegend) to generate monocyte-derived immature DCs. On day 3, one half of the culture medium was replaced with fresh medium containing growth factors as described above. To induce DC maturation, on day 6 of the cell culture, LPS (100 ng/mL, Millipore Sigma) was added for 24 hours. After treatment, DCs were washed in 1x PBS (Thermo Fisher Scientific) and used for subsequent experiments.

Antibodies, flow cytometry, and cell sorting

Monoclonal antibodies specific for CD3 (UCHT1), CD4 (RPA-T4), CD8 (HIT8a), CD28 (CD28.2), CD25 (BC96), ICOSL (2D3), CD14 (63D3), HLA-DR (L243), CD11C (3.9), CD80 (2D10), CD86 (BU63), CD83 (HB15e), human IgG1 Fc (QA19A42), GITR (108-17), CD154 (24–31), CD69 (FN50), ICOS (C398.4A), mouse IgG1 k istotype control (MOPC-21), mouse IgG2b k isotype control (MPC-11), mouse IgG2a k isotpe control (MOPC-173), and Armenian Hamster IgG isotype control (HTK888) were purchased from BioLegend. Monoclonal antibodies specific for ICOS (ISA-3), mouse IgG1 k isotype control (P3.6.2.8.1), were purchased from Thermo Fisher Scientific. IL12 (p40/p70) blocking antibody (C8.6) and mouse IgG1 k isotype control antibody (107.3) were purchased from BD Biosciences. Single-cell suspensions were prepared from human PBMCs or cell lines. The cells were incubated with 2.5 μg of human Fc block (BD Biosciences, 564219) in 100 μL of FACS buffer (1× PBS + 2% FBS + 1 mmol/L EDTA) for 20 minutes on ice followed by staining with the desired fluorochrome-conjugated antibodies for 30 minutes on ice using the same FACS buffer. No washing step is needed between the Fc blocking and staining steps. After washing two times with the FACS buffer described above, cells were analyzed using an M Fortessa X-20 HTS flow cytometer (BD Biosciences). Data analysis was performed using FlowJo software (Tree Star). GFP^+ cells were sorted using a FACSAria SORP UV cell sorter (BD Biosciences). Sorted cells were of >98% purity, as determined by post sort analysis.

Comparison of ICOS-FL and the ICOS splice variant

Two isoforms of human ICOS have been previously identified, the ICOS-FL (1) and the ICOS splice variant (ICOS-SV; ref. 12). The cDNA and 5′UTR sequences of the two ICOS isoforms were searched via Ensembl genome browser (http://useast.ensembl.org/Homo_sapiens/Info/Index). The Ensembl transcript accession numbers (ID) for ICOS-FL and ICOS-SV are ENST00000316386.11 and ENST00000435193.1, respectively; the Ensembl transcript names for ICOS-FL and ICOS-SV are ICOS-201 and ICOS-202, respectively. A comparison was performed in parallel between the two isoforms using Nucleotide BLAST software (https://blast.ncbi.nlm.nih.gov/Blast.cgi?PROGRAM=blastn&BLAST_SPEC=GeoBlast&PAGE_TYPE=BlastSearch) in terms of cDNA sequences and 5′UTR sequences of the two ICOS isoforms. The amino acid sequences of the two ICOS isoforms were searched via UniProt (https://www.uniprot.org/). The UniProt accession numbers (ID) for ICOS-FL and ICOS-SV are Q9Y6W8-1 and Q9Y6W8-2, respectively. A comparison was performed in parallel between these two isoforms using Protein BLAST software (https://blast.ncbi.nlm.nih.gov/Blast.cgi?PROGRAM=blastp&PAGE_TYPE=BlastSearch&BLAST_SPEC=&LINK_LOC=blasttab&LAST_PAGE=blastp).

Two isoforms of human ICOS cloning and construction of retroviral vectors of ICOS-FL and ICOS-SV

$CD3^+$ pan-T cells were purified from the PBMCs of healthy donors by negative selection using a human pan-T cell isolation kit (Miltenyi Biotec, 130-096-535) and MACS separation columns (Miltenyi Biotec, 130-042-401) following the manufacturer's instructions (Miltenyi Biotec). The components of the MACS buffer: 1× PBS (pH 7.2, Thermo Fisher Scientific), 0.5% BSA (Millipore Sigma), 2 mmol/L EDTA (Thermo Fisher Scientific). The purity of the isolated $CD3^+$ pan-T cells was above 95%, determined by flow cytometry. The purified pan-T cells were activated by anti-CD3 (BioLegend, clone UCHT1) and anti-CD28 (BioLegend, clone CD28.2) for 48 hours. The final concentration of anti-human CD3 and anti-human CD28 used was 5 μg/mL each. Total RNA from stimulated T cells was isolated with the RNeasy Mini Kit (Qiagen). cDNA was prepared by oligo-dT primer using the Superscript III Transcription kit (Invitrogen, Thermo Fisher Scientific). The transcript for the ICOS variant was amplified by PCR with the following primers: Forward primer-5′ATGAAGTCAGGCCTCTGGTATTTC3'; Reverse primer-5′GAGTTCCATATTATAGGGTCACATCTT3'. The transcript of the ICOS-FL was amplified by PCR with the primers: Forward primer-5′ATGAAGTCAGGCCTCTGGTATTTC3'; Reverse primer-5′ GAGTTCCATATTATAGGGTCACATCTGTGA3'. The PCR products were inserted into a TA TOPO Vector 4 (Invitrogen) for DNA sequencing analysis (Eton Bioscience, Inc.). The primer used for the DNA sequencing was: 5′ GTAAAACGACGGCCAGT 3′ synthesized from Eton Bioscience. The cDNA of the ICOS-SV and ICOS-FL were further cloned separately into a retroviral expression vector,

MSCV-IRES-GFPII (pMIG II), a gift from Dr. Dario Vignali (Addgene plasmid #52107; http://n2t.net/addgene:52107; RRID: Addgene_52107; ref. 24). The sequences of the primers for the splice variant of ICOS were: Forward primer-5′GCACTGAATTCGCCACCATGAAGTCAGGCCTCTGGTATT3'. Reverse primer-5′GCACTCTCGAGTCACATCTTTTTTGTAAGCCAACAAA3'. The sequences of the primers for the full-length of ICOS were: Forward primer-5′GCACTGAATTCGCCACCATGAAGTCAGGCCTCTGGTATT3'; Reverse primer-5′GCACTCTCGAGTTATAGGGTCACATCTGTGAGTCTAGAT3'. The cloning restriction sites are EcoRI/XhoI.

Retroviral and lentiviral transduction

To produce retrovirus, the pMSCV-IRES-GFPII (pMIG II) expressing splice variant of ICOS or ICOS-FL was cotransfected into 293T cells with envelope vector encoding VSV-g and packaging vector encoding gag/pol using lipofectamine 2000 (Invitrogen). The parental empty retroviral vector was used to produce retrovirus as a negative control. All retroviral supernatants were harvested, filtered, and infected into target cells in the presence of 8 μg/mL polybrene (TR-1003-G, Millipore Sigma). The pLV-GFP-ICOSL lentiviral expression vector was obtained from Sino Biological. Lentiviral supernatants were produced by transfection of 293T cells with the lentiviral vector and envelop/packaging vectors encoding VSV-g, gag/pol, and REV/RSV using lipofectamine 2000 (Invitrogen, Thermo Fisher Scientific). Lentiviral supernatants were harvested and filtered with a 0.45-μm filter. CHO-K1 cells were infected with the ICOSL lentivirus in the presence of 8 μg/mL polybrene (Sigma-Aldrich).

ICOS-SV-fc fusion protein

ICOS-Va-Fc was a fusion protein consisting of human ICOS-Va and a fragment (CH2–CH3 domains) of the constant region (Fc) of human IgG1 (hIgG1, gene ID: 3500). CH2 and CH3 domains are located in the Fc of the hIgG1 heavy chain. The DNA insert encoding ICOS-Va-Fc was made by overlap extension PCR method in which the hIgG1 Fc region was fused to the C-terminus of ICOS-Va. The first DNA fragment (ICOS-Va) was amplified by PCR using ICOS-Va cDNA as template, one pair of primers used for the PCR were designed as follows: ICOS-Va-Forw-EcoRI: 5′GCACTGAATTCGCCACCATGAAGTCAGGCCTCTGGTATT3', ICOS-Va-Fc-Rev-Lig: 5′AGTTTTGTCACAAGATTTGGGCATCTTTTTTGTAAGCCAA3'. The second DNA fragment (hIgG1 Fc) was amplified by PCR using a hIgG1 Fc fusion plasmid (24) as a template; the pair of primers used for this PCR were designed as follows: ICOS-Va-Fc-Forw-Lig: 5′TTGGCTTACAAAAAAGATGCCCAAATCTTGTGACAAAACT3'; Fc-Rev-XhoI: 5′GTACACTCGAGTCATTTACCCGGAGACAGGGA 3′. The two PCR DNA fragments were then purified with a PCR purification kit (Qiagen). To fuse the two DNA fragments, 2 μL of each of purified PCR products was mixed as a template, and the third PCR was performed by using primer ICOS-Va-Forw-EcoRI and primer Fc-Rev-XhoI as described above. The fused insert was cloned into the pMSCV-IRES-GFP II (pMIG II) retroviral vector with EcoRI/XhoI cloning sites to construct recombinant plasmid MSCV/ICOS-Va-Fc for expression of ICOS-Va-Fc fusion protein. The ICOS-Va-Fc was transduced into CHO-K1 cells with 30 μL undiluted retroviral supernatant in the presence of 8 μg/mL polybrene (TR-1003-G, Millipore Sigma). The ICOS-Va-Fc fusion protein was purified using protein G Sepharose 4 Fast Flow according to the manufacturer's instructions (17061801, Cytiva). The buffers used for the Fc fusion protein purification were as follows: binding/washing buffer: 20 mmol/L sodium phosphate, pH7.0; elution buffer: 0.1M glycine-HCl, pH2.7; neutralizing buffer: 1M Tris-HCl, pH9.0. Purified protein was further verified by SDS-PAGE (4%–12% Bis-Tris gradient gel, Invitrogen), immunoblotting, and gel staining was performed using a Pierce silver stain kit according to the manufacturer's instructions (24612, Thermo Fisher Scientific). After staining, the gel was analyzed with ChemiDoc MP Imaging System (Bio-Rad).

Soluble ICOS-SV blocking assays

To evaluate the blocking function of sICOS-SV on ICOS/ICOSL-mediated T-cell costimulation, $CD4^+$ T cells were isolated from PBMCs of healthy donors by negative selection using $CD4^+$ T-cell isolation kit (Miltenyi Biotec, 130-096-533) and MACS separation columns (Miltenyi Biotec, 130-042-401) according to the manufacturer's instructions (Miltenyi Biotec). The components of the MACS buffer: 1× PBS (pH 7.2, Thermo Fisher Scientific), 0.5% BSA (Millipore Sigma), and 2 mmol/L EDTA (Thermo Fisher Scientific). The purity of the isolated $CD4^+$ cells was above 95%, determined by flow cytometry. Purified T cells were cultured in the RPMI-1640 medium (11875093, Thermo Fisher Scientific) supplemented with 10% FBS (Thermo Fisher Scientific, 10437028), 100 U/mL penicillin, and 100 μg/mL streptomycin (Thermo Fisher Scientific, 15140122) and stimulated with a suboptimal dose of monoclonal anti-CD3 (UCHT1, BioLegend) at 20 ng/mL for 24 hours. The T cells were then cocultured with ICOSL-expressing CHO-K1 cells in the presence of either control Ig (110-HG-100, R&D Systems), PD-1 Ig (1086-PD, R&D Systems), or ICOS-SV Ig for 24 hours. Both control Ig and PD-1 Ig were used as negative control.

To determine if sICOS-SV Ig can block the binding membrane-bound ICOS on T cells with sICOSL Ig, $CD3^+$ pan-T cells were purified from the PBMCs of healthy donors by negative selection using a human pan-T cell isolation kit (Miltenyi Biotec, 130-096-535) and MACS separation columns (Miltenyi Biotec, 130-042-401) following the manufacturer's instructions (Miltenyi Biotec) as described above. The components of the MACS buffer: 1× PBS (pH 7.2, Thermo Fisher Scientific), 0.5% BSA (Millipore Sigma), 2 mmol/L EDTA (Thermo Fisher Scientific). The purity of the isolated $CD3^+$ pan-T cells was above 95%, determined by flow cytometry. The purified $CD3^+$pan-T cells were cultured in the RPMI-1640 medium (11875093, Thermo Fisher Scientific) supplemented with 10% FBS (Thermo Fisher Scientific, 10437028), 100 U/mL penicillin, and 100 μg/mL streptomycin (Thermo Fisher Scientific, 15140122) and stimulated with anti-CD3 (UCHT1, BioLegend) at 5 μg/mL for 48 hours. The activated T cells were stained with control Ig (0.2 μg) or ICOSL Ig (0.2 μg) in the presence of buffer, excess ICOS-SV Ig (2 μg) or PD-1 Ig (2 μg) for 30 minutes on ice. After washing three times with FACS buffer (1× PBS + 2% FBS + 1 mmol/L EDTA), the T cells were then incubated with a fluorochrome-conjugated anti-human IgG1 Fc (M1310G05, BioLegend) or isotype control antibody (RTK2758, BioLegend) in 100 μL of FACS buffer for 30 minutes on ice (25). After washing two times with the FACS buffer as described above, cells were analyzed using an M Fortessa X-20 HTS flow cytometer (BD Biosciences). Data analysis was performed using FlowJo software (Tree Star).

Immunoprecipitation, SDS-PAGE, and immunoblotting

Cell culture supernatants from 293T cells transduced with the recombinant retroviral vector encoding either ICOS-SV, ICOS-FL, empty retroviral vector, or from 293T cells parental cells were collected and concentrated with a 3K cutoff centriprep spin column (EMD Millipore). Samples were normalized by cell numbers. The concentrated supernatant was incubated with 10 μg of anti-ICOS (clone C398.4A, BioLegend) plus an 80 μL aliquot of 50% protein A agarose slurry (Thermo Fisher Scientific) overnight at 4°C. After washing with

PBS, the precipitates bound to the agarose beads were resuspended in Laemmli's reducing buffer (Boston Bioproducts), followed by boiling for 5 minutes. Immuno-precipitates were subjected to 4%–12% SDS-polyacrylamide gel electrophoresis (PAGE; Thermo Fisher Scientific) and transferred onto PVDF membranes (EMD Millipore). The membranes were immunoblotted overnight at 4°C with a goat anti-human ICOS at 0.2 mg/mL (R&D Systems) and further incubated with horseradish peroxidase (HRP)-conjugated donkey anti-goat IgG secondary antibody (Jackson ImmunoResearch) at room temperature for 1 hour. The immunoreactive proteins were detected by enhanced chemiluminescence (ECL) reagents (GE Healthcare) and ImageQuant LAS 4000 Imager (GE Healthcare).

For immunoblot analysis, cells were lysed in radioimmunoprecipitation assay (RIPA) buffer (Thermo Fisher Scientific) supplemented with protease inhibitor cocktail (Sigma-Aldrich) or plus phosphatase inhibitor cocktail (Pierce) for phosphorylated proteins. Lysates (40 μg) were separated on NuPAGE 4%–12% Bis-Tris gel (Thermo Fisher Scientific) and transferred onto PVDF membrane (EMD Millipore). Nonspecific binding was blocked by incubation in a blocking buffer (5% nonfat milk in TBST), followed by incubation with the primary antibodies (1:2,000 dilution) and the appropriate HRP-conjugated secondary antibodies (1:5,000 dilution) diluted in the blocking buffer. Immunoreactive proteins were detected using enhanced chemiluminescence (ECL) reagents (GE Healthcare) and ImageQuant LAS 4000 Imager (GE Healthcare). The polyclonal goat anti-human ICOS was purchased from R&D Systems. Rabbit monoclonal antibody for Phospho-Akt (S473), mouse monoclonal antibody for pan-Akt, secondary anti-rabbit IgG-HRP, and secondary anti-mouse IgG-HRP were purchased from Cell Signaling Technology. Secondary anti-goat IgG-HRP was purchased from Jackson ImmunoResearch.

Allogeneic one-way mixed lymphocyte reaction and ^{3}H thymidine proliferation assay

To evaluate the biological function of monocyte-derived DCs (MoDC), a mixed lymphocyte reaction (MLR) was performed in 96-well round-bottom plates by coculturing mitomycin C (Millipore Sigma)-treated MoDCs (50 μg/mL for 45 minutes) as stimulator cells and allogeneic naïve T cells purified with a $CD4^{+}$ T isolation kit (Miltenyi Biotec, 130-096-533, as described above) as responder cells. The ratio of the stimulator cells to responder cells was 1:5 in the coculture. After 6 days of cell culture with the complete RPMI-1640 medium at 37°C, 5% CO_2, cells were pulsed with thymidine (TdR) (0.5mCi/well, PerkinElmer) for the last 15 hours of culture, and the incorporated radioactivity was examined in a liquid scintillation counter (cpm = counts per minute, Wallac 1450 Microbeta Trilux, PerkinElmer) for determination of T-cell proliferation. Soluble (s) ICOS levels were detected by enzyme-linked immunosorbent assay (ELISA) in MLR supernatants as described below. To evaluate the effects of IL12 cytokine produced by GM-CSF/IL4-driven DCs on the ICOS expression of MLR T cells, anti-IL12 p70/p40 (C8.6, BD biosciences) was added to the MLR reaction with GM-CSF/IL4-driven DCs for 24 hours. The working concentration was 10 μg/mL. The purified mouse IgG1 k isotype control (MOPC-31C, BD Biosciences) was used as negative control.

Sera and plasma samples of melanoma patients

A total of 151 Sera and plasma samples were obtained from melanoma patients in the ECOG phase II randomized trial E1608 sponsored by NCI (NCT01134614) comparing ipilimumab plus sargramostim with ipilimumab alone (21). Inclusion and exclusion criteria, such as demographic, geographic, and clinic characteristics, were established for the study participants. The patients' baseline characteristics, including age, weight, sex, and pathologic stage, have been summarized. Sera and plasma were processed from the peripheral blood of the patients in the ECOG-ACRIN Immunology Reference Laboratory at the University of Pittsburgh Cancer Center. Sera and plasma were collected by centrifugation and stored in a monitored −80°C freezer. Specimens were analyzed via ELISA from 78 patients receiving ipilimumab plus sargramostim (arm A) and 73 patients receiving ipilimumab (arm B used as control; **Table 1**).

Table 1. Number of patients in each group by treatment arms in the E1608 clinical trial.

Group	Arm A ($N = 78$)	Arm B ($N = 73$)	Overall ($N = 151$)
sICOS ratio group			
High	29 (37.2%)	26 (35.6%)	55 (36.4%)
Low	49 (62.8%)	47 (64.4%)	96 (63.6%)
sICOS pregroup			
High	40 (51.3%)	35 (48.0%)	75 (50.0%)
Low	38 (48.7%)	38 (52.0%)	76 (50.0%)

Note: Patients were divided into two groups according to post-/preratio (high/low) or pretreatment baseline levels (high/low).

To deplete sICOS protein from patient serum samples with a high abundance of sICOS, 12 μL of serum sample was diluted to 90 μL with 1× PBS and incubated with 3 μg of ICOS monoclonal antibody (C398.4A, BioLegend) for 2 hours at 4°C to form an immune complex. The solution containing the immune complex was then added to the immunoaffinity protein G Sepharose spin column (Previously equilibrated in 1× PBS; 28903134, Cytiva) and incubated at room temperature for 1 hour. The column was centrifuged at 10,000 rpm for 1 minute, and the flow-through fraction representing the sICOS-depleted serum was collected in a clean tube. Samples were further concentrated with Vivaspin 500 centrifugal concentrator (28932218, Cytiva) to the original volume. To keep other components the same as in the depleted serum samples, the control serum samples without depletion of sICOS were processed with the same procedures as described above, except for replacing the incubation of the ICOS monoclonal antibody with the incubation of the purified Armenian Hamster IgG isotype control (HTK888, BioLegend).

ELISA

To evaluate soluble ICOS-SVs in the sera of melanoma patients or cell culture supernatants, the Human ICOS DuoSet ELISA kit (DY169, R&D Systems) was used according to the manufacturer's protocol. In brief, for sICOS in patient samples, 4 μg/mL of anti-ICOS capture antibody (R&D Systems) was coated on Costar ELISA plates (Corning) overnight at 4°C. The plates were then washed with PBS supplemented with 0.05% Tween-20 three times and blocked with protein-free blocking buffer (Pierce) for 6 hours. Patient sera or plasma were diluted with PBS in a 1:1 volume ratio. 100 μL of the diluted patient sample was added to each well and incubated overnight at 4°C. Plates were then washed with PBS containing 0.05% Tween-20 six times and incubated with 100 ng/mL of the biotinylated anti-ICOS detection antibody (R&D Systems) in the protein-free blocking buffer for 2 hours at room temperature. Plates were then washed with PBS containing 0.05% Tween-20 six times and incubated with streptavidin-HRP (R&D Systems) diluted 1:200 in protein-free blocking buffer for 1 hour at room temperature. After washing with PBS containing 0.05%

Tween-20 six times, plates were developed by adding TMB (Pierce). Samples were read at an optical density (OD) of 450 nm on a Spectramax M3 microplate reader (Molecular Devices Corp). All samples were assayed in duplicate. A standard curve with recombinant human ICOS was performed with each assay. For sICOS in cell supernatants: 4 μg/mL of anti-ICOS capture antibody (R&D Systems) was coated on Costar ELISA plates (Corning) overnight at 4°C. The plates were then washed with PBS supplemented with 0.05% Tween-20 three times and blocked with protein-free blocking buffer (Pierce) for 6 hours. Cell supernatants were diluted with PBS in a 1:1 volume ratio. 100 μL of the diluted samples was added to each well and incubated overnight at 4°C. Plates were then washed with PBS containing 0.05% Tween-20 six times and incubated with 100 ng/mL of the biotinylated anti-ICOS detection antibody (R&D Systems) in the protein-free blocking buffer for 2 hours at room temperature. Plates were then washed with PBS containing 0.05% Tween-20 six times and incubated with streptavidin–HRP (R&D Systems) diluted 1:200 in protein-free blocking buffer for 1 hour at room temperature. After washing with PBS containing 0.05% Tween-20 six times, plates were developed by adding TMB (Pierce). Samples were read at an OD of 450 nm on a Spectramax M3 microplate reader (Molecular Devices Corp). All samples were assayed in duplicate. A standard curve with recombinant human ICOS was performed with each assay.

To determine human IL12 p40, IL12p70, TNFα, and IFNγ in cell culture supernatants, IL12 p40 (430701), IL12 p70 (431701), TNFα (430201), and IFNγ (430101) ELISA kits purchased from BioLegend were used according to the manufacturer's protocols, respectively. In brief, each of the capture antibodies against the proteins (BioLegend) above was 1:200 diluted with PBS in 100 μL volume/well and coated on Costar ELISA plates (Corning) overnight at 4°C. The plates were then washed with PBS supplemented with 0.05% Tween-20 three times and blocked with protein-free blocking buffer (Pierce) for 2 hours. Cell culture supernatants were diluted with PBS in a 1:1 volume ratio. 100 μL of the diluted sample was added to each well and incubated 2 hours at 4°C. Plates were then washed with PBS containing 0.05% Tween-20 six times and incubated with the corresponding biotinylated detection antibody (BioLegend) 1:200 diluted in the protein-free blocking buffer for 1 hour at room temperature. Plates were then washed with PBS containing 0.05% Tween-20 four times and incubated with streptavidin–HRP (BioLegend) diluted 1:1000 in protein-free blocking buffer for 0.5 hours at room temperature. After washing with PBS containing 0.05% Tween-20 four times, plates were developed by adding TMB (Pierce). Samples were read at an OD of 450 nm on a Spectramax M3 microplate reader (Molecular Devices Corp). All samples were assayed in duplicate. A standard curve with recombinant human IL12-p40, IL12-p70, TNFα, or IFNγ was performed with each assay, respectively.

Statistical analysis

ELISAs were performed in duplicate to determine sICOS levels in patient serum samples and culture supernatants. Clinical data were obtained from the ECOG1608 trial (21). Kaplan–Meier plots, along with log-rank tests, were used to compare overall survival (OS) and progression-free survival (PFS) between different sICOS ratio groups. The Fisher exact test was used to compare overall response and nonprogressive response. For the sICOS ratio of post/pretreatment, the cutoff values of post-/preratio were explored from median to 75% quantile with 0.1 increments to dichotomize the ICOS ratio as high versus low, and 2.2 as the cutoff value was selected. Patients' samples were taken before treatment and 3 months posttreatment. All statistical analysis was performed with Prism software 9.2.0 (GraphPad) and statistical significance was determined where the *P* value was less than *, 0.05; **, 0.01; ***, 0.001; ****, 0.0001, or ns, not significant, when the *P* value was more than 0.05. Standard deviation (SD) is shown in the graphs. A two-tailed paired *t* test was used for comparison of two groups with paired samples. A two-tailed unpaired *t* test was used for comparison of two unpaired groups. A one-way ANOVA was used for single comparisons with more than two groups.

Data availability

The data generated in this study are available in the article and its supplementary data files, or upon reasonable request from the corresponding author.

Results

Comparison between ICOS-FL and ICOS-SV

Two isoforms of human ICOS have been previously identified, the ICOS-FL (1) and the ICOS-SV (12). The cDNA sequences of the two ICOS isoforms, amino acids, and 5′UTR were searched via the Ensembl genome browser and UniProt. A comparison was performed in parallel between these two isoforms. The human ICOS-FL consists of 5 exons and encodes a 199 amino acid protein, and the transmembrane domain (TM) is located in exon 3 (**Fig. 1A**). ICOS-SV harbors a 96-base pair (bp) deletion from nucleotide (nt) 569 to nt 664 of ICOS, followed by a 3-bp addition, which removes 32 out of 38 amino acid residues in the C-terminal end of the intracellular domain and adds one additional residue of methionine to the end of the protein (**Fig. 1B**). The splice occurs from the end of exon 3 (encodes the TM domain) to the beginning of exon 5, deleting entire exon 4 and part of exon 5, resulting in the removal of most of the cytoplasmic domain. Furthermore, the 5′UTR of ICOS-SV lacks 32 nucleotides compared with the 5′UTR of ICOS-FL.

Secretion of the ICOS-SV

To determine whether the ICOS-SV is a secreted or membrane-bound protein, the cDNAs of human ICOS-SV and ICOS-FL were cloned via RT-PCR with total RNA isolated from healthy volunteer's peripheral activated T cells (**Fig. 2A**). The cDNAs were constructed into a bicistronic GFP retroviral vector and pMSCV-IRES-EGFPII (pMIG II), respectively. The cDNA sequences of ICOS-FL and ICOS-SV were validated by Sanger sequencing (**Fig. 2B** and **C**). 293T cells, which lack endogenous ICOS, were transduced with the recombinant retroviral vector encoding either ICOS-SV or ICOS-FL. GFP^+ cells were sorted via FACS, and purified cells transduced with different retroviral vectors were obtained. Sorted GFP^+ cells were cultured to assess cell growth and expansion. Subsequently, immunoblot analysis, ELISA, immunoprecipitation (IP)-SDS-PAGE-immunoblot, and flow cytometry analyses were conducted with the sorted GFP^+ cells. ICOS-FL–overexpressing cells exhibited a very strong ICOS protein signal compared with ICOS-SV-overexpressing cells or empty vector–transduced cells (**Fig. 2D**). In comparison, ICOS-SV–overexpressing cells showed a dim ICOS protein signal with smaller molecular weight than that of ICOS-FL due to its truncation. A sandwich ELISA assay was conducted to determine if ICOS protein can be secreted into the supernatant of the cultured 293T cells transduced with the ICOS-SV retroviral vector. Supernatant collected from the cells transduced with GFP-empty lentiviral vector was used as a negative control. A high concentration of the sICOS-SV protein was detected in culture supernatants from ICOS-SV–overexpressing cells. However, sICOS protein was undetectable in the supernatants of negative control and ICOS-FL–overexpressing cells (**Fig. 2E**).

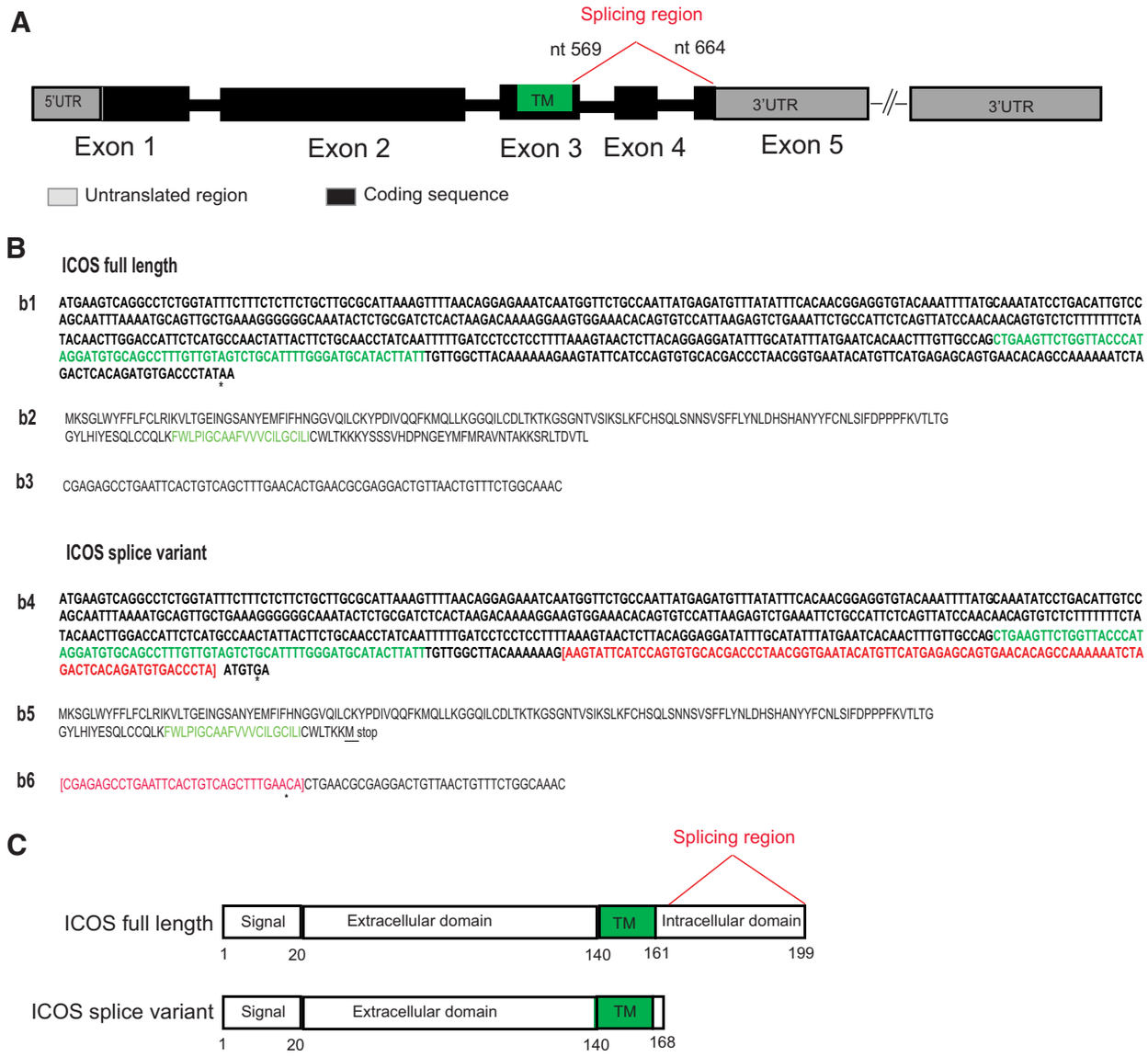

Figure 1.

Comparison between human ICOS full length and splice variant. **A,** Schematic representation of full length and spliced variant of human ICOS. The full length of ICOS consists of 5 exons. The gray boxes denote untranslated regions, and the black boxes denote coding sequences. The transmembrane domain (TM) is located in exon 3 and labeled with a green bar. The splicing region is shown in red. **B,** Comparison of cDNA nucleotide sequences, amino acid sequences, and 5′UTR sequences between ICOS-FL and the splice variant. Nucleotide sequences of cDNA for ICOS-FL (b1) and the splice variant of ICOS (b4) are represented; spliced region of ICOS is shown in red and delineated by red brackets; the nucleotides and amino acids of TM are shown in green. Asterisk indicates the stop codon. Amino acid sequences of full length of ICOS (b2) and the splice variant of ICOS (b5) are shown. The underline depicts additional differences in amino acid sequence compared with ICOS-FL. "Stop" represents a stop codon. 5′UTR sequences of ICOS-FL (b3) and the splice variant of ICOS (b6) are shown. The 5′UTR of the ICOS-SV lacks 32 nucleotides compared with the 5′UTR of ICOS-FL shown in red and delineated by red brackets. **C,** Schematic diagram of ICOS-FL and the ICOS-SV protein. Thirty-two out of 38 amino acids in the intracellular domain are spliced, as shown in red.

Moreover, an immunoprecipitation-immunoblot assay was performed to confirm ICOS-SV protein in the culture supernatants. Truncated ICOS-SV was detected in ICOS-SV–overexpressing cells, but no protein was detected in the supernatants derived from the negative control and ICOS-FL–overexpressing cells (**Fig. 2F**). In addition, we investigated whether residual ICOS-SV could be detected and quantified the protein abundance on the cell surface by flow cytometry using 293T cells transduced with ICOS-SV retroviral vector. The 293T cells transduced with ICOS-FL or empty retroviral vector were used as positive control and negative control, respectively. The fluorescence intensity of surface ICOS on the cells transduced with ICOS-FL was significantly higher compared with negative control. In contrast, the fluorescence intensity on the cells transduced with ICOS-SV was significantly less than the ICOS-FL–transduced cells (Supplementary Fig. S1A and S1B). Taken together, these results indicated that the majority of ICOS-SV can be secreted extracellularly.

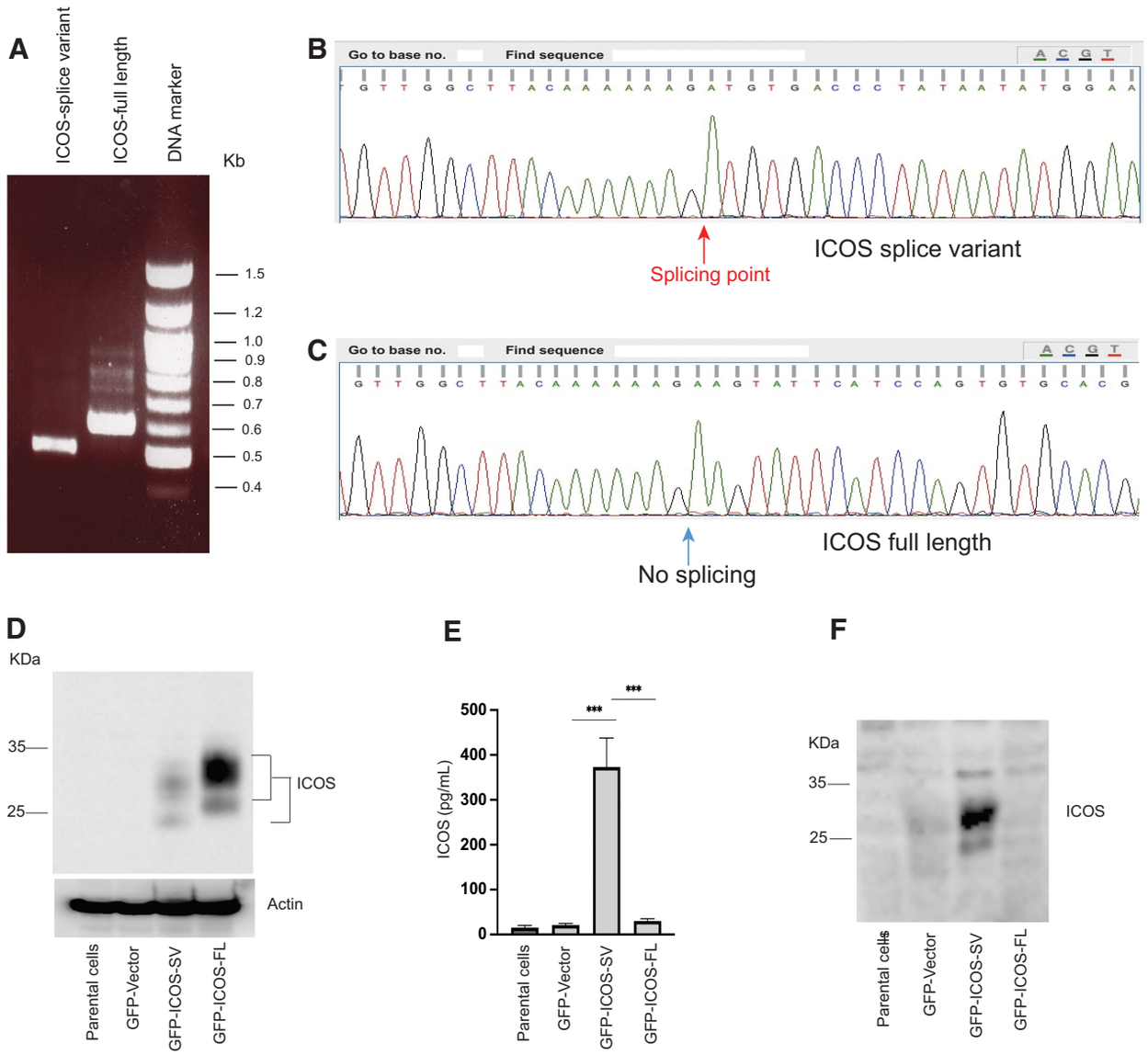

Figure 2.

Secretion of the ICOS-SV from ICOS-SV–overexpressing cells. **A,** RT-PCR to detect the ICOS-SV in human T cells. Total RNA was isolated from purified T cells in PBMCs of a healthy donor. Expression of the ICOS variant was examined by RT-PCR with specific primers. RT-PCR of ICOS-FL is shown as a control. **B,** DNA sequencing of ICOS-SV cDNA from human T cells. The cDNA of the PCR product was cloned into a TOPO TA vector. The ICOS-SV was confirmed by DNA sequencing using an M13 forward primer. Splicing point is shown by the red arrow. **C,** DNA sequencing of ICOS-FL cDNA is shown as a control. No splicing occurs in the region corresponding to the position in (**B**), as shown in blue. **D,** Expression of ICOS-SV and ICOS-FL in 293T cells determined by immunoblot. 293T cells were transduced with recombinant GFP retroviral vector encoding either ICOS-SV or ICOS-FL as a positive control. The parental cells and the GFP-empty vector–transduced cells were used as negative controls. Sample loading was normalized to actin. **E,** Cell culture supernatants were collected from the cells described in (**A**). Secreted ICOS-SV was examined by ELISA. Two-tailed unpaired *t* test was used to compare ICOS secretion between the two groups. ***, $P < 0.001$. Standard deviation of the mean (SD) is shown. **F,** To validate the secreted ICOS variant protein in the cell supernatant, immunoprecipitation, SDS-PAGE, and immunoblotting assays were performed. Sample loading was normalized to cell numbers.

Suppressive effects of sICOS-SV on T-cell costimulation via the ICOS/ICOSL axis

Soluble ICOS-SV is capable of binding ICOSL (ICOS ligand) on cells and competes with membrane-bound ICOS for binding to ICOSL, thereby inhibiting T-cell proliferation. To study this, a retroviral vector overexpressing an ICOS-SV-Fc fusion protein was constructed, and the recombinant Fc fusion protein, ICOS-SV Ig, was successfully purified (Supplementary Fig. S2). In addition, ICOSL-negative CHO-K1 cells were transduced with either ICOSL-expressing lentiviral vector or empty lentiviral vector as a control, and expression of ICOSL on the cell surface was examined by flow cytometry. ICOSL was highly detectable in transduced CHO-K1 cells (**Fig. 3A**). Next, the binding capacity of sICOS-SV Ig, control Ig, or PD-1 Ig to ICOSL-expressing CHO-K1 cells was evaluated by flow cytometry. Soluble control Ig was used as a negative control and PD-1 Ig was used as another negative control because it does not bind to ICOSL. Soluble

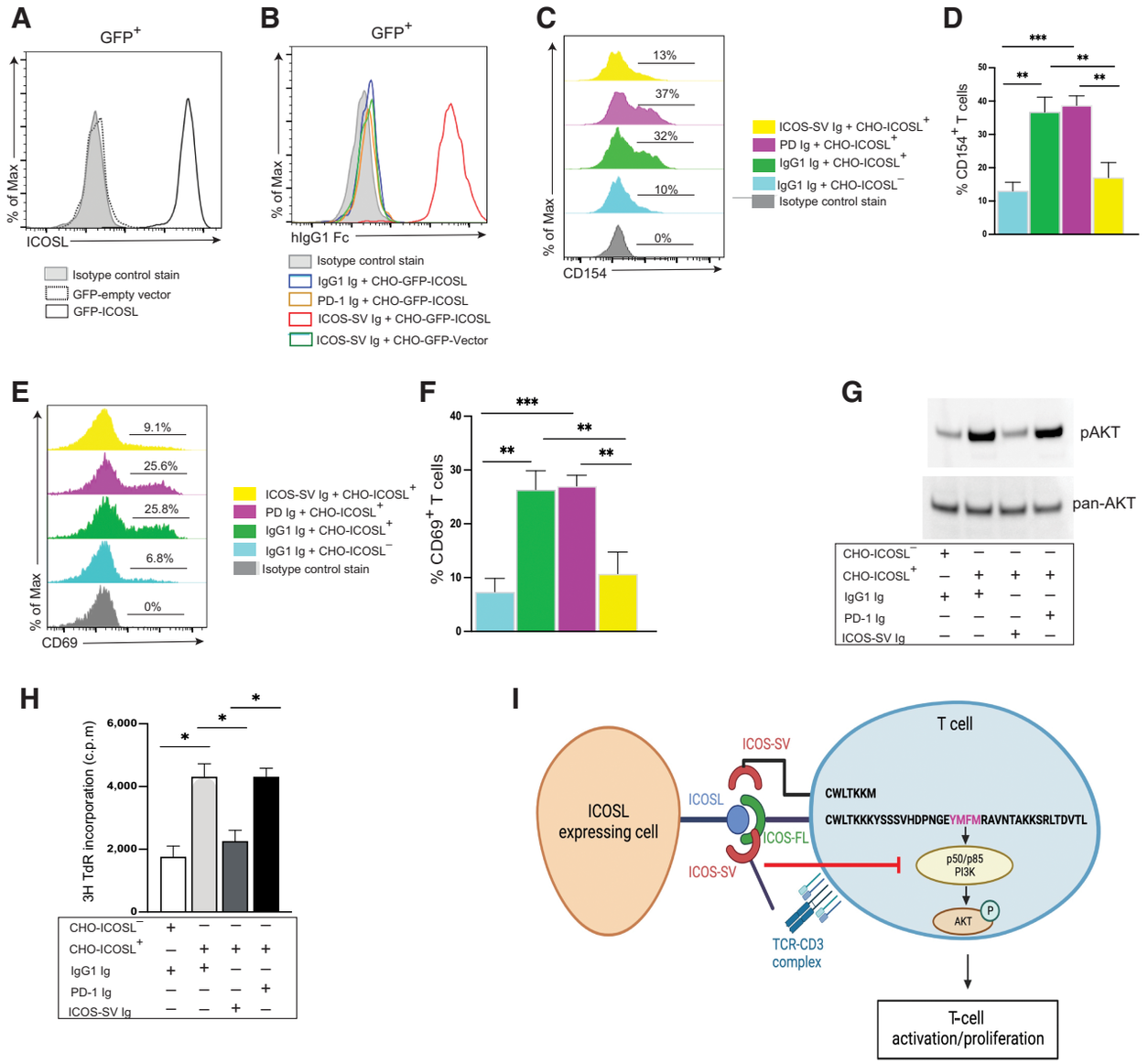

Figure 3.

Suppressive effects of sICOS-SV on the costimulation of T cells. **A,** CHO-K1 cells were transduced with either ICOSL-expressing lentiviral vector or GFP-empty vector (CHO-ICOSL$^-$) as a negative control. Expression of ICOSL on the cell surface of CHO-K1 was examined by flow cytometry using anti-ICOSL (open histogram with solid line) or lentivirus GFP-empty vector (open histogram with dotted line). Isotype antibody was used as a negative control (filled histogram). **B,** ICOSL-expressing CHO-K1 cells were stained with ICOS-SV Ig (red line), control IgG Ig (blue line), or PD-1 Ig (orange line) and analyzed by flow cytometry. Both soluble control Ig and PD-1 Ig were used as negative controls. GFP-empty vector-expression CHO-K1 cells stained with ICOS-SV Ig (green line) were used as another negative control for the binding assay. Isotype antibody control was used as a negative control (gray filled histogram). **C,** CD154 expression was determined by FACS analysis. Isotype control antibody is shown in gray. Activated T cells treated with a suboptimal dose of anti-CD3 were incubated with control Ig + CHO-ICOSL$^-$ cells (CHO cells transduced with GFP-empty vector, blue), control Ig + CHO-ICOSL$^+$ cells (green), PD-1 Ig + CHO-ICOSL$^+$ cells (red), or ICOS-SV Ig + CHO-ICOSL$^+$ cells (yellow). Both control Ig and PD-1 Ig were used as negative controls. **D,** Two-tailed unpaired *t* test was used to compare expression of CD154 between two groups. **, $P < 0.01$; ***, $P < 0.001$. Standard deviation of the mean (SD) is shown. **E,** CD69 expression was determined by FACS analysis. Isotype control antibody is shown in gray. Activated T cells treated with a suboptimal dose of anti-CD3 were incubated with control Ig + CHO-ICOSL$^-$ cells (CHO cells transduced with GFP-empty vector, blue), control Ig + CHO-ICOSL$^+$ cells (green), PD-1 Ig + CHO-ICOSL$^+$ cells (red), or ICOS-SV Ig + CHO-ICOSL$^+$ cells (yellow). Both control Ig and PD-1 Ig were used as negative controls. **F,** Two-tailed unpaired *t* test was used to compare expression of CD69 between the two groups. **, $P < 0.01$; ***, $P < 0.001$. Standard deviation of the mean (SD) is shown. **G,** CHO cells transduced with GFP-empty vector (CHO-ICOSL$^-$) were used as negative controls. Sample loading was normalized to total pan-Akt. **H,** T-cell proliferation was determined by a [^{3}H]-TdR thymidine incorporation assay. CHO cells transduced with empty vector (CHO-ICOSL$^-$) were used as negative controls. Two-tailed unpaired *t* test was used to compare ^{3}H uptake between the two groups, respectively. *, $P < 0.1$. Standard deviation of the mean (SD) is shown. **I,** Schematic diagram of ICOS/ICOSL costimulatory T-cell proliferation, as well as the blocking function of the sICOS-SV. Depicted are the cytoplasmic tail sequences of ICOS-FL and sICOS-SV isoforms. The YMFM Src Homology 2 (SH2) binding motif in the cytoplasmic tail of the ICOS-FL is highlighted in pink. Upon ICOS engagement by the ICOSL on CHO cells, the unique YMFM motif recruits a p85a and a p50a subunits of PI3K, resulting in the elevated phosphorylation of Akt, thereby inducing PI3K activity. In contrast, the ICOS-SV, a truncated isoform lacking the YMFM motif in its cytoplasmic tail, cannot elicit phosphorylation of Akt. Consequently, it fails to promote T-cell proliferation. The secreted ICOS-SV (red) competes with membrane-bound ICOS for binding to ICOSL, thereby blocking the interaction between ICOSL and membrane ICOS. As a result, the sICOS-SV suppresses phosphorylation of Akt and T-cell proliferation, leading to the inhibition of T-cell immunity. The diagram was created with BioRender.com. All data shown are representative of at least 2 independent experiments.

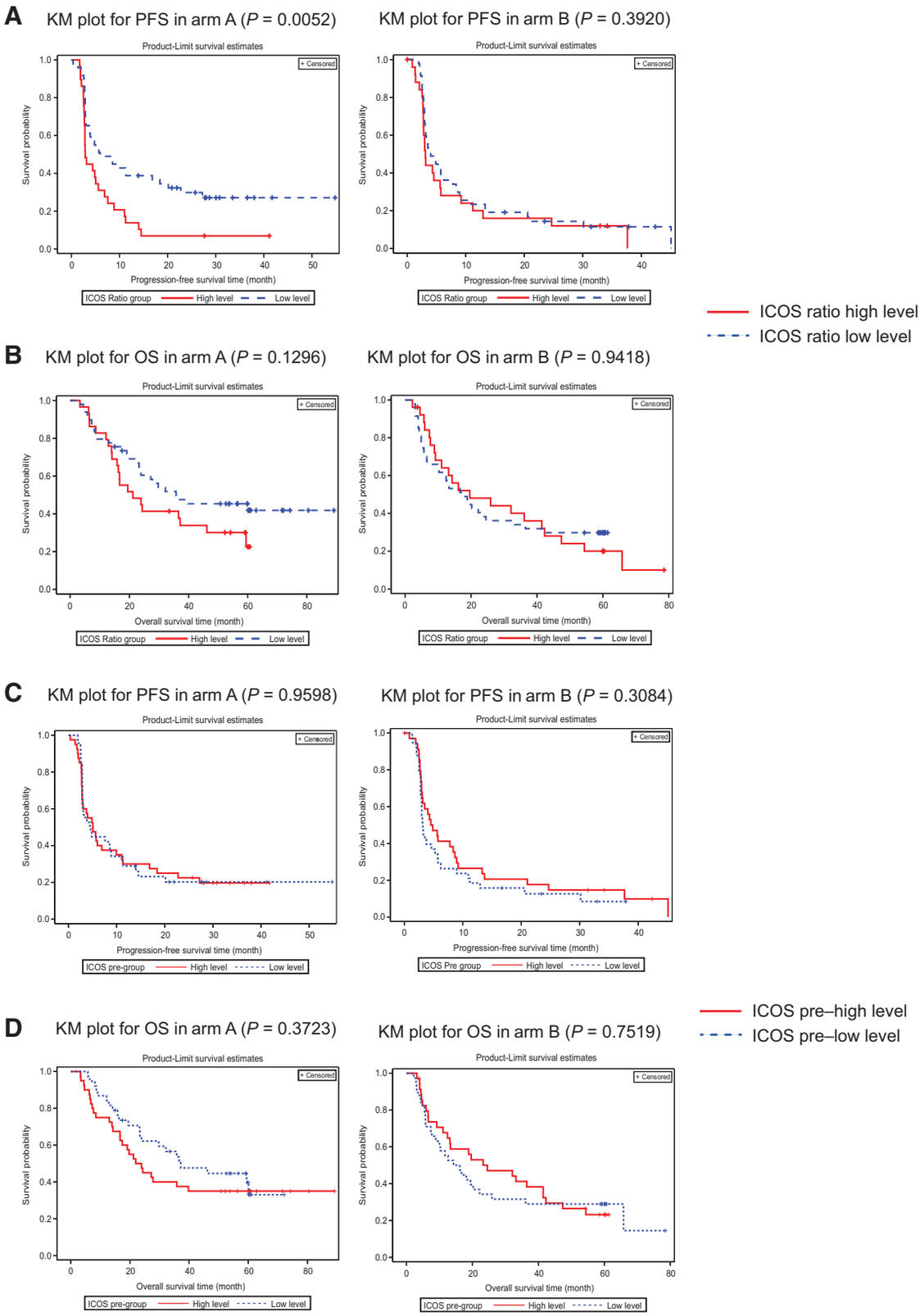
A
KM plot for PFS in arm A (P = 0.0052)
KM plot for PFS in arm B (P = 0.3920)
B
KM plot for OS in arm A (P = 0.1296)
KM plot for OS in arm B (P = 0.9418)
C
KM plot for PFS in arm A (P = 0.9598)
KM plot for PFS in arm B (P = 0.3084)
D
KM plot for OS in arm A (P = 0.3723)
KM plot for OS in arm B (P = 0.7519)
Product-Limit survival estimates
+ Censored
Survival probability
Progression-free survival time (month)
Overall survival time (month)
ICOS Ratio group
ICOS pre-group
ICOS Pre group
High level
Low level
ICOS ratio high level
ICOS ratio low level
ICOS pre–high level
ICOS pre–low level

ICOS-SV Ig, but not control Ig or PD-1 Ig, could specifically bind to cell-surface ICOSL (**Fig. 3B**). Additionally, sICOS-SV Ig specifically blocked the binding of ICOSL to cell-surface ICOS induced on activated T cells isolated from healthy donor PBMCs (Supplementary Fig. S3).

To investigate the effects of sICOS-SV Ig on T-cell costimulation induced by ICOS/ICOSL engagement, T cells were purified from human PBMCs of healthy donors and stimulated with a suboptimal dose of monoclonal anti-CD3 for 24 hours for the induction of membrane-bound ICOS. The activated T cells were then cocultured with ICOSL-expressing CHO-K1 cells in the presence of either control Ig, PD-1 Ig, or ICOS-SV Ig. PD-1 Ig was used as the second negative control instead of CTLA-4 Ig because CTLA-4 has been reported to bind to ICOSL (26). The functional effects of ICOS-SV Ig on CD154 (CD40 ligand), CD69, phosphorylation of PI3K/Akt, and T-cell proliferation were determined by flow cytometry analysis, immunoblot, and incorporation of [^{3}H] TdR, respectively. Upregulation of CD154, CD69, PI3K/pAkt, and T-cell proliferation induced by ICOS/ICOSL signaling pathway was eliminated by ICOS-SV Ig, but not control Ig or PD-1 Ig, indicating that the competition of ICOS-SV Ig was specific (**Fig. 3C–H**). These data indicate that sICOS-SV Ig inhibits ICOS/ICOSL axis-mediated costimulatory effects on T cells. To summarize the ICOS/ICOSL costimulatory T-cell proliferation and the blocking function of the sICOS-SV on this pathway, a schematic diagram was drawn (**Fig. 3I**).

Changes in sICOS correlate with clinical outcomes in melanoma patients treated with ipilimumab plus GM-CSF but not ipilimumab alone

We next investigated the immunologic function and characterization of sICOS-SV and assessed whether the changes in sICOS had clinical significance in melanoma patients treated with ipilimumab plus GM-CSF versus ipilimumab alone. We previously reported that upregulation of membrane ICOS expression on peripheral CD4$^+$ and CD8$^+$ T cells was greater in the patients treated with GM-CSF plus ipilimumab (arm A) versus ipilimumab alone (arm B; ECOG 1608; ref. 21), suggesting that GM-CSF enhances membrane ICOS expression on T cells. Here, to study how GM-CSF influenced the sICOS isoform in melanoma patients, plasma specimens from 78 patients at pretreatment and 3 months posttreatment in arm A and from 73 patients in arm B were evaluated to assess the relationship between sICOS ratio (post/pre) and PFS and OS (**Table 1**). In arm A, but not arm B, the sICOS ratio (post/pre) dichotomized at 2.2 negatively correlated with PFS ($P = 0.0052$; **Fig 4A**). Similarly, in arm A, but not arm B, there is a trend toward a negative correlation between sICOS ratio (cutoff 2.2) and OS ($P = 0.1296$; **Fig. 4B**). Our data suggest that patients in arm A with increased sICOS ratios had poorer clinical outcomes. To evaluate if pretreatment sICOS affected clinical outcomes, PFS and OS for the E1608 clinical trial were analyzed in the context of baseline sICOS (high vs. low). Kaplan–Meier plots for PFS or OS and corresponding *P* values in each arm are shown in **Fig. 4C** and **D**, respectively. This result indicated that the baseline sICOS levels did not correlate with clinical outcomes in the clinical trial (**Fig. 4C** and **D**). The median PFS and OS for patients in the E1608 trial are listed in Supplementary Table S1.

GM-CSF plays an essential role in the differentiation and development of MoDCs

Previous findings (21) prompted us to investigate the mechanism by which GM-CSF promoted T-cell activation/proliferation and induced membrane-bound ICOS expression in T cells. GM-CSF is known to play an important role in DC development, and it has been investigated in various model systems with different precursor cell types (17, 27, 28). Here, an MLR was used to evaluate T-cell reactivity and ICOS induction by allogeneic MoDCs generated by GM-CSF/IL4. First, we investigated whether GM-CSF/IL4 had a stimulatory effect on the differentiation and development of immature DCs (iDC) *in vitro*, which served as the prerequisite for downstream experiments evaluating allogenic T-cell reactivity. CD14$^+$ monocytes were purified with magnetic beads from human PBMCs isolated from the peripheral blood of healthy donors and cultured *in vitro* with GM-CSF + IL4 for 6 days. The Mo-iDCs were matured with LPS for 24 hours. On day 7, costimulatory molecules CD80, CD86, mature DC marker CD83, and ICOSL were assessed. Gating on the CD14$^-$HLA-DR$^+$CD11c$^+$ cells, the expression of CD80, CD86, and CD83 in GM-CSF/IL4–driven DCs was much higher than that in control monocytes (Supplementary Fig. S4A–S4F). To verify the specificity of GM-CSF's impact on the generation of MoDCs, anti-CD116 (GM-CSF receptor alpha) was added to the purified CD14$^+$ monocytes in the presence of GM-CSF/IL4. Anti-CD116 abrogated the effects of GM-CSF on the development of DCs (Supplementary Fig. S4A–S4F). Significantly higher levels of IL12p70 (Supplementary Fig. S4G) and IL12p40 (Supplementary Fig. S4H) were detected in the supernatants of GM-CSF/IL4-driven DCs compared with control and anti-CD116–treated cells. To determine if ICOSL expression could be regulated by GM-CSF in the DCs, we determined cell-surface ICOSL protein levels on CD14$^-$HLA-DR$^+$CD11C$^+$ cells by flow cytometry. Our data showed that ICOSL was not upregulated by GM-CSF (Supplementary Fig. S5).

GM-CSF enhances membrane-bound ICOS expression on T cells and promotes T-cell priming by DCs

To evaluate T-cell activation in the MLR assays, the expression of membrane-bound ICOS, GITR, and CD25 on the activated CD4$^+$T cells was examined by flow cytometry. Purified CD4$^+$ from PBMCs, used as "responders," were cocultured with various allogeneic DCs (control DCs, GM-CSF/IL4 + hIgG-driven DCs, GM-CSF/IL4 + anti-CD116–driven DCs) serving as "stimulators" for 6 days. GM-CSF/IL4 + hIgG-driven DCs induced significantly higher levels of ICOS, GITR, and CD25 expression on CD4$^+$ T cells compared with control DCs (**Fig. 5A** and **B**). The allogeneic DCs generated by GM-CSF/IL4 + anti-CD116 showed similar effects on T-cell activation compared with control DCs.

Figure 4.

Kaplan–Meier (KM) survival curves for PFS and OS in the E1608 clinical trial. **A,** KM plot for the correlation between progression-free survival (PFS) and sICOS ratio (post/pre) for patients in arm A and arm B of the E1608 clinical trial. Left, red curve represents 29 patients; blue curve represents 49 patients. Right, red curve represents 26 patients; blue curve represents 47 patients. **B,** KM plot for the correlation between overall survival (OS) and sICOS ratio (post/pre) for patients in the E1607 trial. Left, red curve represents 29 patients; blue curve represents 49 patients. Right, red curve represents 26 patients; blue curve represents 47 patients. **C,** KM plot for the correlation between PFS and sICOS pretreatment baseline levels in arm A ($P = 0.9598$) and arm B ($P = 0.3084$). Left, red curve represents 40 patients; blue curve represents 38 patients. Right, red curve represents 35 patients; blue curve represents 38 patients. **D,** KM plot for the correlation between OS and sICOS pretreatment baseline levels in arm A ($P = 0.3723$) and arm B ($P = 0.7519$). Left, red curve represents 40 patients; blue line curve represents 38 patients. Right, red curve represents 35 patients; blue curve represents 38 patients. Log-rank was used for PFS and OS analysis. Arm A: ipilimumab + GM-CSF treatment group; arm B: ipilimumab-alone treatment group. The cutoff value of the sICOS ratio (post-/pretreatment) was 2.2.

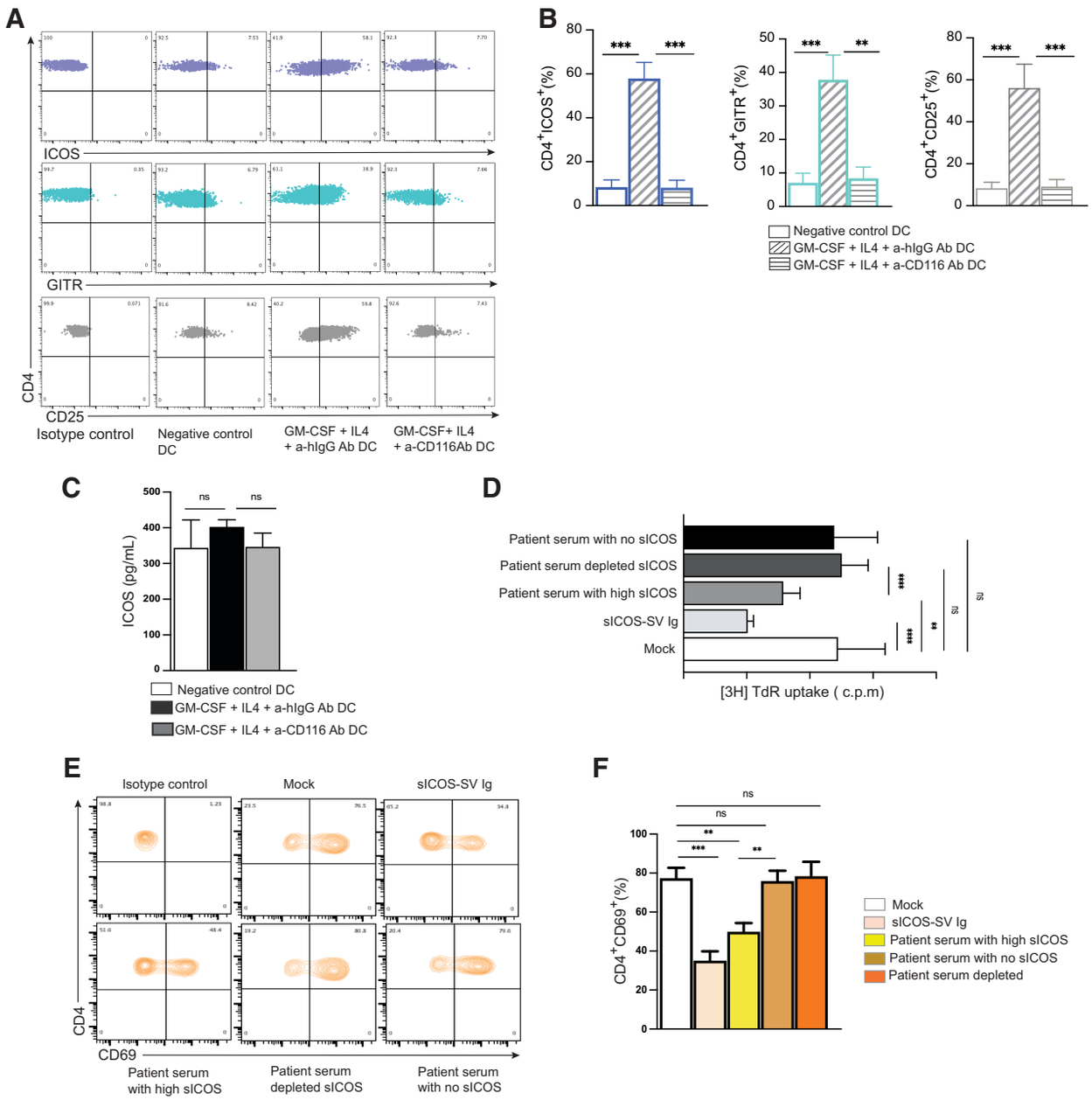

Figure 5.

sICOS from melanoma patients inhibits T-cell activation and proliferation induced by GM-CSF–driven DCs in MLRs. **A,** $CD4^+$ T cells (responders) were stimulated by allogeneic GM-CSF–driven MoDCs (stimulators: negative control DCs, DCs generated by GM-CSF/IL4 + anti-IgG, or DCs generated by GM-CSF/IL4 + anti-CD116) in MLRs. T cells were assessed for activation via flow cytometry using anti-ICOS (blue), anti-GITR (green), or anti-CD25 (gray). Isotype control antibodies were used as negative controls. **B,** Statistical analysis of the percentage of $CD4^+ICOS^+$, $CD4^+GITR^+$, and $CD4^+CD25^+$ T-cell populations from different groups as described above. **C,** Soluble ICOS levels were determined by ELISA using supernatants from the MLRs described above. **D–E,** Serum from sICOS-high and sICOS-negative patients were added to the MLRs, and T-cell proliferation (**D**) and CD69 expression (**E**) were evaluated. Additionally, sICOS was depleted from sICOS-high serum to assess its effects on T cells. **F,** Statistical analysis of the percentage of $CD4^+CD69^+$ T-cell populations from different groups as described above. All data shown are representative of at least 2 independent experiments. Two-tailed unpaired *t* test was used between the two groups. **, $P < 0.01$; ***, $P < 0.001$; ****, $P < 0.0001$; ns, not significant ($P > 0.05$). Standard deviation of the mean (SD) is shown.

To evaluate the impact of IL12 produced by GM-CSF/IL4–driven-DCs on ICOS expression by allogenic $CD4^+$ T cells, blocking anti-IL12 (p70/p40) was administered in the MLR assay of GM-CSF/IL4-driven DC group. The results show that ICOS expression was reduced in the presence of anti-IL12 compared with the control group (Supplementary Fig. S6A). IFNγ and TNFα secretion was significantly greater in MLRs containing GM-CSF/IL4–driven DCs than those with other DCs (Supplementary Fig. S6B–S6C). To determine if GM-CSF/IL4–driven

DCs induced sICOS levels in $CD4^+$ T cells from the MLRs, ELISAs were performed. Soluble ICOS was increased with GM-CSF/IL4–driven DCs compared with the other DCs, but was not statistically significant ($P > 0.05$; **Fig. 5C**).

Next, the allogeneic proliferation of T cells by GM-CSF/IL4–driven DCs was examined in the MLRs. The allogeneic stimulator cells (DCs) were treated with mitomycin C before coculturing with T cells. Cells were pulsed with [^{3}H] TdR. Allogeneic GM-CSF/IL4–driven DCs induced T-cell proliferation compared with control DCs, and anti-CD116 almost completely suppressed the ability of GM-CSF/IL4–driven DCs to induce allogeneic T-cell proliferation (Supplementary Fig. S6D).

We further investigated whether the ICOS/ICOSL axis was involved in allogeneic T-cell proliferation, CD69 activation, and IFNγ secretion elicited by GM-CSF/IL4–driven DCs. To address this, sICOS-SV Ig was used in the MLR assays. ICOS-SV Ig significantly inhibited T-cell proliferation as determined by [^{3}H] TdR incorporation (**Fig. 5D**), CD69 expression by flow cytometry (**Fig. 5E** and **F**), and IFNγ production by ELISA (Supplementary Fig. S6E). We also examined if sICOS from the sera of patients with melanoma showed similar results. A representative patient's serum with a high concentration of sICOS and a representative patient's serum negative for sICOS were added to the above MLRs, respectively. Serum with high sICOS exhibited a significant inhibitory effect on T-cell activation, similar to that obtained by the addition of sICOS-SV Ig (**Fig. 5E** and **F**; Supplementary Fig. S6E). In contrast, a negligible inhibition was observed when the patient's serum was negative for sICOS. Moreover, to highlight the immunomodulatory capacity of serum sICOS from patients with melanoma, serum with high sICOS levels was sICOS-depleted and then used in the MLR assays. The depleted serum was ineffective at inhibiting T-cell responses induced by GM-CSF–driven DCs, as measured by [^{3}H] TdR incorporation, flow cytometry, and ELISA. These findings suggest that the ICOS/ICOSL axis constitutes a critical costimulatory signaling pathway in the alloreactive T-cell responses and that sICOS from patient serum is able to inhibit T-cell stimulation.

Discussion

Although the alternatively spliced variant of ICOS was previously identified (12), an improved understanding of its subcellular location, biological effects, immunologic function, and clinical impact on cancer immunotherapy is needed. In the current study, we demonstrated that the majority of ICOS-SV can be secreted extracellularly, which is consistent with the assertion in the UniProtKB (Q9Y6W8) stating it is a secretory protein, whereas a minority remains on the cell surface. Nevertheless, the minority of surface ICOS-SV would be nonfunctional for T-cell activation and proliferation because the ICOS-SV is a truncated isoform lacking the YMFM motif in its cytoplasmic tail. The YMFM motif has been shown to play an important role in enhancing PI3K activity and T-cell activation (29, 30). In general, alternative splicing of membrane proteins can cause an altered reading frameshift and creates a premature stop codon before the transmembrane domain, thereby resulting in the secretion of splice variants (24, 31–34). In this ICOS variant, lacking most of the intracellular domain due to splicing also results in secretion, implying that the intracellular domain plays an important role in stabilizing ICOS on the cell surface. A possible biological mechanism by which ICOS-SV with a transmembrane domain can be secreted includes a protein conformational change due to the truncation of the cytoplasmic domain, resulting in glycosylation and secretion. Likewise, our recent study identified several secreted, soluble PD-L1 splice variants (24). In one of the variants, named PD-L1-1, the splicing takes place in the cytoplasmic tail following the TM domain. The resulting PD-L1-1 variant isoform has a truncated short cytoplasmic tail and is expressed in both secreted and membrane-bound forms (24).

ICOS-FL is a type I transmembrane glycoprotein containing an extracellular immunoglobulin domain, a transmembrane domain, and a cytoplasmic tail. Despite the overall similarity in the T-cell costimulatory function between ICOS and CD28, ICOS exerts specific functions on immune responses (1, 4, 5, 29, 30). The FDPPPF consensus sequence located in the extracellular domain of ICOS is essential for ICOSL-specific binding (1), whereas the MYPPPY consensus sequence, which is not conserved in ICOS, is involved in the binding of CD28 and CTLA-4 to B7-1 (CD80)/B7-2 (CD86; ref. 35). ICOS-FL possesses the unique YMFM Src Homology 2 (SH2) binding motif in its cytoplasmic tail. Upon ICOS ligation by the ICOSL, the YMFM motif recruits a p85a catalytic subunit and a p50a regulatory subunit of PI3K. Interestingly, ICOS ligation has been shown to preferentially recruit the p50a to the immunologic synapse over the p85a subunit (5, 29), leading to the increased phosphorylation of Akt, and thereby inducing PI3K activity. Similarly, CD28 has a YMNM SH2 binding motif in the cytoplasmic tail. Although both ICOS and CD28 costimulation can activate the PI3K–Akt axis, ICOS/ICOSL engagement is more robust than the CD28/B7 interaction in its capacity to augment phosphorylation of Akt and PI3K activity (29, 30). The PI3K/Akt signaling pathway is important for T-cell growth and immune responses (36, 37). Thus, costimulation mediated by the ICOS/ICOSL pathway is a potent activator and enhances T-cell activation, proliferation, and survival, which has been evidenced in previous investigations (4, 38, 39).

In contrast to ICOS-FL, ICOS-SV, a truncated isoform lacking the YMFM motif in its cytoplasmic tail, would not be able to elicit the phosphorylation of Akt and PI3K activity and would fail to promote T-cell proliferation and survival, even if the variant is partially expressed on the cell membrane. We investigated the immunoregulatory effects of sICOS in multiple signaling pathways. Our data demonstrated that sICOS-SV competes with membrane-bound ICOS for binding to ICOSL, thereby blocking the interaction between ICOSL and the cell-surface ICOS-FL and significantly abrogates the upregulation of CD154, CD69, Akt phosphorylation/PI3K activity, and T-cell proliferation induced by the ICOS/ICOSL interaction, resulting in inhibition of T-cell immunity.

In the current study, the circulating ICOS-SV ratios of post-/pretreatment in patients with advanced melanoma treated with GM-CSF in combination with immune checkpoint blockade (arm A) correlated with survival outcomes but did not correlate in patients treated with immune checkpoint blockade alone (arm B). The mechanism may involve sICOS-SV blocking activity to inhibit costimulation via the ICOS/ICOSL axis. Although GM-CSF in combination with IL4 is used conventionally for the generation of MoDCs *in vitro*, it has been reported that GM-CSF plays an essential role in the differentiation of DC, whereas IL4 is known as an inhibitor of macrophage colony formation, allowing optimal DC growth and differentiation (40). GM-CSF enhanced IL12 cytokine production by MoDCs, as well as the antigen-presenting potency of DCs, reflected by the upregulation of membrane ICOS, GITR, and CD25 expression on the allo-stimulatory T cells, increased IFNγ and TNFα production, and the increased T-cell activity. Due to the limitations of using PBMCs from the ECOG clinical trial, further cellular analyses from patient samples, such as the determination of the membrane ICOS on peripheral T cells, were not permitted.

GM-CSF was able to enhance membrane-bound ICOS expression but not sICOS-SV. GM-CSF exerts its biological functions through binding to the GM-CSF receptor (GM-CSFR), a member of the type I cytokine receptor superfamily composed of alpha and beta subunits. The GM-CSF alpha chain is the major GM-CSF–binding subunit and is specific for GM-CSF (41). CD116 antibody was capable of fully blocking DC differentiation and maturation generated by GM-CSF/IL4, as indicated by the downregulated expression of costimulatory molecules, such as CD80, CD86, and CD83. In addition, administration of the CD116 antibody suppressed T-cell proliferation, inhibited IFNγ and TNFα production, and downregulated membrane-bound ICOS, GITR, and CD25 expression on the alloreactive T cells after MLR, suggesting that GM-CSF can specifically promote membrane-bound ICOS induction on T cells via enhancing DC development and differentiation. Moreover, IL12 has been reported to enhance cell-surface ICOS expression on activated human $CD4^+$ T cells (42). Therefore, we proposed that GM-CSF could increase surface ICOS expression levels through IL12 secreted by DCs. When IL12-neutralizing antibody was added to the GM-CSF/IL4 MLR cell cultures, surface ICOS expression was significantly downregulated compared with the isotype-matched control antibody group, suggesting that GM-CSF's effect on the membrane-bound form of ICOS is partially dependent on IL12.

In the present study, serum derived from melanoma patients with high sICOS-SV levels blocked T-cell proliferation induced by MLR. This supports the possible immunoregulatory functions of ICOS-SV *in vivo*. Clinical correlates revealed that changes in the soluble ICOS-SV were associated with patient outcomes in patients receiving GM-CSF. The regulation of sICOS on T cells could be critical for the mechanisms of sICOS-mediated immunosuppression that contribute to clinical outcomes. It is important to further investigate if regulatory T cells or exhausted T effectors generate increased sICOS levels compared with activated effector T cells. Although these analyses are limited to a single data set in one clinical trial, data warrant further investigation into sICOS-SV as a potential marker for GM-CSF cytokine-directed treatments, as a prognostic biomarker for immunotherapy and as a potential target for future combinatorial approaches.

Authors' Disclosures

L.H. Butterfield reports LHB Advisory activities (honoraria): Calidi Scientific and Medical Advisory Board, April 6, 2017–present; KaliVir, Scientific Advisory Board, 2018–present; Torque Therapeutics, Scientific Advisory Board, 2018–2020; Khloris, Scientific Advisory Board, 2019–present; Pyxis, Scientific Advisory Board, 2019–present; CytomX, Scientific Advisory Board, 2019–present; DCprime, Scientific Advisory Board meeting, Nov. 2020; RAPT, Scientific Advisory Board, 2020–present; Takeda, Scientific Advisor, 2020–present; EnaraBio scientific advisor, Feb. 2021; Federation Bio scientific advisor Sept.–Oct. 2022; Pfizer scientific advisor Oct 2022; Apple tree 2022–present; Orionis 2023. G. Dranoff reports other support from Novartis Pharmaceuticals during the conduct of the study; other support from Novartis Pharmaceuticals outside the submitted work; and employee and stockholder of Novartis Pharmaceuticals. F.S. Hodi reports other support from CTEP/NIH during the conduct of the study; personal fees from Bristol Myers Squibb, Merck, Novartis, Surface, Compass Therapeutics, Apricity, Bicara, Checkpoint Therapeutics, Genentech/Roche, Bioentre, Gossamer, Iovance, Catalym, Immunocore, Kairos, Rheos, Zumutor, Corner Therapeutics, Curis, and Astra Zeneca outside the submitted work; in addition, F.S. Hodi has a patent for "Methods for Treating MICA-Related Disorders" (#20100111973) pending, a patent for tumor antigens and uses thereof (#7250291) issued, a patent for "Angiopoiten-2 Biomarkers Predictive of Anti-immune checkpoint response" (#20170248603) pending, a patent for "Compositions and Methods for Identification, Assessment, Prevention, and Treatment of Melanoma using PD-L1 Isoforms" (#20160340407) pending, a patent for therapeutic peptides (#20160046716) pending, a patent for methods of using pembrolizumab and trebananib pending, a patent for vaccine compositions and methods for restoring NKG2D pathway function against cancers (#10279021) issued, a patent for antibodies that bind to MHC class I polypeptide-related sequence A (#10106611) issued, and a patent for anti-galectin antibody biomarkers predictive of anti-immune checkpoint and anti-angiogenesis responses (#20170343552) pending. No disclosures were reported by the other authors.

Authors' Contributions

X. Li: Conceptualization, data curation, formal analysis, validation, investigation, visualization, methodology, writing–original draft, project administration, writing–review and editing. **J. Li:** Data curation, validation, investigation, visualization, methodology. **Y. zheng:** Data curation, software, formal analysis, validation, investigation, writing–review and editing. **S.J. Lee:** Data curation, software, formal analysis, validation, investigation, writing–review and editing. **J. Zhou:** Data curation, validation, investigation, visualization, methodology, writing–review and editing. **A. Giobbie-Hurder:** Data curation, software, formal analysis, validation, investigation, writing–review and editing. **L.H. Butterfield:** Resources, writing–review and editing. **G. Dranoff:** Conceptualization, investigation, visualization, writing–review and editing. **F.S. Hodi:** Conceptualization, resources, data curation, formal analysis, supervision, funding acquisition, validation, investigation, visualization, methodology, writing–original draft, project administration, writing–review and editing.

Acknowledgments

Samples were provided by ECOG and supported in part by Public Health Service Grants CA23318, CA66636, CA21115, CA80775, CA39229, CA49957, and CA32291 and by the NCI, NIH and the Department of Health and Human Services. Its contents are solely the responsibility of the authors and do not necessarily represent the official views of the NCI. Support for clinical trial E1608 was provided by Sanofi Company and Bristol Myers Squibb. Research support was given by the E. Michael Egan Melanoma Research Fund, Jane and Brian Crowley Melanoma Research Fund, Martin, Fideli, Mitchell Fund for Melanoma and Immuno-Oncology Research, Malcolm and Emily MacNaught Fund for Melanoma Research, and Christin Holbrook Harding Fund for Melanoma Research.

The publication costs of this article were defrayed in part by the payment of publication fees. Therefore, and solely to indicate this fact, this article is hereby marked "advertisement" in accordance with 18 USC section 1734.

Note

Supplementary data for this article are available at Cancer Immunology Research Online (http://cancerimmunolres.aacrjournals.org/).

Received September 8, 2022; revised January 3, 2023; accepted May 23, 2023; published first June 1, 2023.

References

1. Hutloff A, Dittrich AM, Beier KC, Eljaschewitsch B, Kraft R, Anagnostopoulos I, et al. ICOS is an inducible T-cell co-stimulator structurally and functionally related to CD28. Nature 1999;397:263–6.
2. Buonfiglio D, Bragardo M, Redoglia V, Vaschetto R, Bottarel F, Bonissoni S, et al. The T cell activation molecule H4 and the CD28-like molecule ICOS are identical. Eur J Immunol 2000;30:3463–7.
3. Mages HW, Hutloff A, Heuck C, Buchner K, Himmelbauer H, Oliveri F, et al. Molecular cloning and characterization of murine ICOS and identification of B7h as ICOS ligand. Eur J Immunol 2000;30:1040–7.
4. Yoshinaga SK, Whoriskey JS, Khare SD, Sarmiento U, Guo J, Horan T, et al. T-cell co-stimulation through B7RP-1 and ICOS. Nature 1999;402:827–32.

5. Coyle AJ, Lehar S, Lloyd C, Tian J, Delaney T, Manning S, et al. The CD28-related molecule ICOS is required for effective T cell-dependent immune responses. Immunity 2000;13:95–105.
6. Beier KC, Hutloff A, Dittrich AM, Heuck C, Rauch A, Buchner K, et al. Induction, binding specificity and function of human ICOS. Eur J Immunol 2000;30:3707–17.
7. Swallow MM, Wallin JJ, Sha WC. B7h, a novel costimulatory homolog of B7.1 and B7.2, is induced by TNFalpha. Immunity 1999;11:423–32.
8. Kopf M, Coyle AJ, Schmitz N, Barner M, Oxenius A, Gallimore A, et al. Inducible costimulator protein (ICOS) controls T helper cell subset polarization after virus and parasite infection. J Exp Med 2000;192: 53–61.
9. Sharpe AH, Freeman GJ. The B7-CD28 superfamily. Nat Rev Immunol 2002;2: 116–26.
10. Maurer DM, Adamik J, Santos PM, Shi J, Shurin MR, Kirkwood JM, et al. Dysregulated NF-kappaB-dependent ICOSL expression in human dendritic cell vaccines impairs T-cell responses in patients with melanoma. Cancer Immunol Res 2020;8:1554–67.
11. Fu T, He Q, Sharma P. The ICOS/ICOSL pathway is required for optimal antitumor responses mediated by anti-CTLA-4 therapy. Cancer Res 2011;71: 5445–54.
12. Gerhard DS, Wagner L, Feingold EA, Shenmen CM, Grouse LH, Schuler G, et al. The status, quality, and expansion of the NIH full-length cDNA project: the mammalian gene collection (MGC). Genome Res 2004;14: 2121–7.
13. Xue Q, Li X, Gu Y, Wang X, Wang M, Tian J, et al. Unbalanced expression of ICOS and PD-1 in patients with neuromyelitis Optica Spectrum Disorder. Sci Rep. 2019;9:14130.
14. Hasegawa M, Fujimoto M, Matsushita T, Hamaguchi Y, Takehara K. Augmented ICOS expression in patients with early diffuse cutaneous systemic sclerosis. Rheumatology (Oxford) 2013;52:242–51.
15. Hutloff A, Buchner K, Reiter K, Baelde HJ, Odendahl M, Jacobi A, et al. Involvement of inducible costimulator in the exaggerated memory B cell and plasma cell generation in systemic lupus erythematosus. Arthritis Rheum 2004; 50:3211–20.
16. Yang JH, Zhang J, Cai Q, Zhao DB, Wang J, Guo PE, et al. Expression and function of inducible costimulator on peripheral blood T cells in patients with systemic lupus erythematosus. Rheumatology (Oxford) 2005;44:1245–54.
17. Dranoff G. GM-CSF-based cancer vaccines. Immunol Rev 2002;188:147–54.
18. Hodi FS, Mihm MC, Soiffer RJ, Haluska FG, Butler M, Seiden MV, et al. Biologic activity of cytotoxic T lymphocyte-associated antigen 4 antibody blockade in previously vaccinated metastatic melanoma and ovarian carcinoma patients. Proc Natl Acad Sci U S A 2003;100:4712–7.
19. Hodi FS, Butler M, Oble DA, Seiden MV, Haluska FG, Kruse A, et al. Immunologic and clinical effects of antibody blockade of cytotoxic T lymphocyte-associated antigen 4 in previously vaccinated cancer patients. Proc Natl Acad Sci U S A 2008;105:3005–10.
20. Soiffer R, Hodi FS, Haluska F, Jung K, Gillessen S, Singer S, et al. Vaccination with irradiated, autologous melanoma cells engineered to secrete granulocyte-macrophage colony-stimulating factor by adenoviral-mediated gene transfer augments antitumor immunity in patients with metastatic melanoma. J Clin Oncol 2003;21:3343–50.
21. Hodi FS, Lee S, McDermott DF, Rao UN, Butterfield LH, Tarhini AA, et al. Ipilimumab plus sargramostim vs ipilimumab alone for treatment of metastatic melanoma: a randomized clinical trial. JAMA 2014;312:1744–53.
22. van Elsas A, Hurwitz AA, Allison JP. Combination immunotherapy of B16 melanoma using anti-cytotoxic T lymphocyte-associated antigen 4 (CTLA-4) and granulocyte/macrophage colony-stimulating factor (GM-CSF)-producing vaccines induces rejection of subcutaneous and metastatic tumors accompanied by autoimmune depigmentation. J Exp Med 1999;190:355–66.
23. van den Eertwegh AJ, Versluis J, van den Berg HP, Santegoets SJ, van Moorselaar RJ, van der Sluis TM, et al. Combined immunotherapy with granulocyte-macrophage colony-stimulating factor-transduced allogeneic prostate cancer cells and ipilimumab in patients with metastatic castration-resistant prostate cancer: a phase 1 dose-escalation trial. Lancet Oncol 2012;13:509–17.
24. Zhou J, Mahoney KM, Giobbie-Hurder A, Zhao F, Lee S, Liao X, et al. Soluble PD-L1 as a Biomarker in Malignant Melanoma Treated with Checkpoint Blockade. Cancer Immunol Res 2017;5:480–92.
25. Wang S, Zhu G, Chapoval AI, Dong H, Tamada K, Ni J, et al. Costimulation of T cells by B7-H2, a B7-like molecule that binds ICOS. Blood 2000;96:2808–13.
26. Beyersdorf N, Kerkau T, Hunig T. CD28 co-stimulation in T-cell homeostasis: a recent perspective. Immunotargets Ther 2015;4:111–22.
27. McKenna HJ. Role of hematopoietic growth factors/flt3 ligand in expansion and regulation of dendritic cells. Curr Opin Hematol 2001;8:149–54.
28. Lellahi SM, Azeem W, Hua Y, Gabriel B, Paulsen Rye K, Reikvam H, et al. GM-CSF, Flt3-L and IL-4 affect viability and function of conventional dendritic cell types 1 and 2. Front Immunol 2022;13:1058963.
29. Fos C, Salles A, Lang V, Carrette F, Audebert S, Pastor S, et al. ICOS ligation recruits the p50alpha PI3K regulatory subunit to the immunological synapse. J Immunol 2008;181:1969–77.
30. Parry RV, Rumbley CA, Vandenberghe LH, June CH, Riley JL. CD28 and inducible costimulatory protein Src homology 2 binding domains show distinct regulation of phosphatidylinositol 3-kinase, Bcl-xL, and IL-2 expression in primary human CD4 T lymphocytes. J Immunol 2003;171:166–74.
31. Magistrelli G, Jeannin P, Elson G, Gauchat JF, Nguyen TN, Bonnefoy JY, et al. Identification of three alternatively spliced variants of human CD28 mRNA. Biochem Biophys Res Commun 1999;259:34–7.
32. Venables JP. Aberrant and alternative splicing in cancer. Cancer Res 2004;64: 7647–54.
33. Gower HJ, Barton CH, Elsom VL, Thompson J, Moore SE, Dickson G, et al. Alternative splicing generates a secreted form of N-CAM in muscle and brain. Cell 1988;55:955–64.
34. Tang W, Gunn TM, McLaughlin DF, Barsh GS, Schlossman SF, Duke-Cohan JS. Secreted and membrane attractin result from alternative splicing of the human ATRN gene. Proc Natl Acad Sci U S A. 2000;97:6025–30.
35. Peach RJ, Bajorath J, Brady W, Leytze G, Greene J, Naemura J, et al. Complementarity determining region 1 (CDR1)- and CDR3-analogous regions in CTLA-4 and CD28 determine the binding to B7-1. J Exp Med 1994;180: 2049–58.
36. Uche UU, Piccirillo AR, Kataoka S, Grebinoski SJ, D'Cruz LM, Kane LP. PIK3IP1/TrIP restricts activation of T cells through inhibition of PI3K/Akt. J Exp Med 2018;215:3165–79.
37. Busca A, Saxena M, Iqbal S, Angel J, Kumar A. PI3K/Akt regulates survival during differentiation of human macrophages by maintaining NF-kappaB-dependent expression of antiapoptotic Bcl-xL. J Leukoc Biol 2014; 96:1011–22.
38. Simpson TR, Quezada SA, Allison JP. Regulation of CD4 T cell activation and effector function by inducible costimulator (ICOS). Curr Opin Immunol 2010; 22:326–32.
39. Fruman DA, Chiu H, Hopkins BD, Bagrodia S, Cantley LC, Abraham RT. The PI3K Pathway in Human Disease. Cell 2017;170:605–35.
40. Romani N, Gruner S, Brang D, Kampgen E, Lenz A, Trockenbacher B, et al. Proliferating dendritic cell progenitors in human blood. J Exp Med 1994;180: 83–93.
41. Guthridge MA, Stomski FC, Thomas D, Woodcock JM, Bagley CJ, Berndt MC, et al. Mechanism of activation of the GM-CSF, IL-3, and IL-5 family of receptors. Stem Cells 1998;16:301–13.
42. Wassink L, Vieira PL, Smits HH, Kingsbury GA, Coyle AJ, Kapsenberg ML, et al. ICOS expression by activated human Th cells is enhanced by IL-12 and IL-23: increased ICOS expression enhances the effector function of both Th1 and Th2 cells. J Immunol 2004;173:1779–86.